J. Ocean Univ. China (Oceanic and Coastal Sea Research)
DOI 10.1007/s11802-011-1840-3
ISSN 1672-5182, 2011 10 (4): 305-313
http://www.ouc.edu.cn/xbywb/
E-mail:xbywb@ouc.edu.cn

Doctor Forum

Numerical Study on the Bifurcation of the North Equatorial Current

LIU Yulong[1), 2)], WANG Qi[1), *], SONG Jun[2)], ZHU Xiande[1), 3)], GONG Xiaoqing[1)], and WU Fang[1)]

1) *Department of Marine Meteorology*, *Ocean University of China*, *Qingdao* 266100, *P. R. China*
2) *National Marine Data and Information Service*, *Tianjin* 300171, *P. R. China*
3) *People's Liberation Army* 91422 *Troops*, *Yantai* 265200, *P. R. China*

(Received March 30, 2011; revised May 6, 2011; accepted August 22, 2011)

Abstract A 1.5-layer reduced-gravity model forced by wind stress is used to study the bifurcations of the North Equatorial Current (NEC). The authors found that after removing the Ekman drift, the modelled circulations can serve well as a proxy of the SODA circulations on the σ_θ=25.0 kg m^{-3} potential density surface based on available long-term reanalysis wind stress data. The modelled results show that the location of the western boundary bifurcation of the NEC depends on both zonal averaged and local zero wind stress curl latitude. The effects of the anomalous wind stress curl added in different areas are also investigated and it is found that they can change the strength of the Mindanao Eddy (ME), and then influence the interior pathway.

Keyword North Equatorial Current; the western boundary; interior pathway; bifurcation; wind stress curl; 1&1/2 Model

1 Introduction

The North Equatorial Current (NEC) is an upper westward ocean current flowing to the west boundary of the Pacific. In the east of the Philippines, the NEC bifurcates into the northward Kuroshio Current (KC) and the southward Mindanao Current (MC) (Nitani, 1972; Toole *et al.*, 1990). Hence, the NEC is both the south branch of the subtropical circulation and the north branch of the tropical circulation. The NEC also contributes a great deal to the Western Pacific Warm pool (Qu *et al.*, 1997) in heat budget, which is a key area of the ENSO cycle (Webster and Lukas, 1992). The NEC system at the western boundary flows into the global thermohaline circulation through the Indonesian throughflow directly (Gorden, 1986), which plays an important role in the transport of mass, heat and salt volume in the ocean (Qu *et al.*, 1998). The western Pacific region is an intersection for the formation of water masses at high latitudes (Fine *et al.*, 1994). One of the major roles of the ocean circulation is the meridional redistribution of heat: the warm water is conveyed to the polar region while the cold water moves from the poles toward the equator. Recent studies show that apart from the KC and MC, there is a third way out of the NEC, the interior pathway along which pycnocline water reaches the equator through the interior of the ocean. Thus, there are two bifurcations of the NEC: the western boundary bifurcation and the interior bifurcation. So arises the concept of the subtropical cell: the net heat from the low latitude ocean is transported northward from the surface to the NEC, conveying the net heat to high latitudes by the KC; the cold water of subduction at the middle latitude flows to the south in the thermocline, then the NEC bifurcates into the tropic by different pathways, overturning at the equator and finally forming a shallow meridional overturning circulation (McCreary and Lu, 1994; Liu, 1994; Lu *et al*., 1998; Johnson and McPhaden, 1999; Wang and Liu, 2000). The NEC transports cold water to the equatorial region through the interior of the ocean in the middle Pacific, constituting the interior pathway of the NEC. The interannual and interdecadal variations of the NEC bifurcation can affect the heat distribution and thermal structure in the tropical and subtropical Pacific, and then affect the local or global climate. Therefore, the change of NEC bifurcation point plays a very important role in global climate change.

The NEC of the climatic charater is located at 7°N–16°N (Liu *et al.*, 2003), which is a shallow circulation driven by the wind and buoyancy flux (McCreary and Lu, 1994) with the velocity of the NEC being about 0.2–0.3 m s^{-1} (Ye and Li, 1992). The flow axis of the NEC is from east to west along about 15°N. Because of the topographic barrier, the NEC bifurcates into two currents, the Northward KC and the Southward MC, after it reaches the western boundary at the east coast of the Philippines, where it forms the important sources of the two currents. When the Kuroshio loses its dependence on the continental shelf at the Luzon Strait, it forms a Kuroshio loop in

* Corresponding author. Tel: 0086-532-66782592
E-mail: wangqi@ouc.edu.cn

the strait mouth (Liu *et al.*, 1996; Li *et al.*, 1998a). There are many studies (Dale, 1956; Chu, 1972; Huang, 1983; Li *et al*., 1994; Li *et al*., 1998b; Qu *et al.*, 2000; Metzger and Hurlburt, 2001; Yuan, 2002; Cai *et al*., 2005; Su and Yuan, 2005) on the effects of the Kuroshio on the South China Sea (SCS) and the water exchange. The MC formed by the southward NEC near the Philippines is the source of the Indonesia throughflow (Masumoto and Yamagata, 1991), part of which forms a compensating flow that flows in the opposite direction of the NEC, forming the North Equatorial Countercurrent (NECC) from west to east.

The study of the NEC system in the Pacific has attracted the interest of many scholars as early as in the late 1930's. Schott (1939) pointed out that the NEC off the east coast of the Philippines bifurcated, and presented a simple image of the northward KC and the southward MC for the first time. Wyrtki (1961) studied the current in the Western Pacific region by using the ship data of hydrological observations and described the low latitude western boundary current in the Pacific, and named it the MC. On the basis of the dynamic topography proposed by Takahashi (1959), Wyrtki also named two eddies, *i.e.* the Mindanao Eddy (ME) and the Halmahera Eddy (HE). Later many scholars (Tsuchiya, 1968; Masuzawa, 1968; Lighthill, 1969; Stommel and Yoshida, 1972; Nitani, 1972) did a series of studies on the characteristics of the low latitude western boundary current. Until the 1990's, the studies on the NEC bifurcation was mainly based on very few observations in estimating its bifurcation latitude (Wyrtki, 1961; Nitani, 1972; Kessler and Taft, 1987; Toole *et al*., 1988, 1990). In the late 1990's, as attention increased in the international community, with more funds injected and more data available, many scholars (Qiu and Lukas, 1996; Metzger and Hurlburt, 1996; Qu *et al*., 1998; Wajsowicz, 1999; Qu *et al*., 1999; Qu and Lukas, 2002, 2003; Kim *et al*., 2004; Yaremchuk and Qu, 2004; Li *et al.*, 2005; Wang and Hu, 2006; Zhang *et al.*, 2008; Wang *et al.*, 2009; Qiu and Chen, 2010; Chen and Wu, 2011) turned to this hot topic and many technical means for research were developed. They began to pay attention to the seasonal and interannual variation of the NEC bifurcation.

The trade wind of the North Pacific is located between the subtropical high and the belt of equatorial calm. The characteristics of the wind stress distribution are consistent with the planetary wind system (Li *et al*., 1996), and the wind stress as an important part of ocean-atmosphere interaction, reflects the dynamic effect of the atmosphere which forces ocean circulation. The early theories of Sverdrup (1947), Stommel (1948) and Munk (1950) show that wind stress and its curl play an important role in the formation of ocean circulation, and the mass transport can be studied by the wind stress. When wind stress is irrotational, the upper ocean circulation will disappear. Hence, wind stress is the main driving force in large scale upper ocean circulation.

The NEC bifurcation represents the actual boundaries of subtropical circulation, tropical circulation and tropical inner circulation, so the changes of subtropical circulation and tropical circulation will lead to the changes in the bifurcation state, and the wind stress as the main driving force should be given full consideration. Although there are some high quality ocean assimilation data at present, the fixed data can not be repeated for diagnostic analysis, and it can not be used to conduct sensitivity test for specific regions and variables. The NEC bifurcation point at the western boundary and the interior bifurcation are both of shallow depth as far as the entire ocean is concerned, therefore the effect of wind stress is very significant. Here we use a 1.5-layer reduced-gravity model forced by wind stress for this study.

2 1.5-layer ocean model and data

Many studies (Han, 1984; Zeng *et al*., 1985; Wang and Su, 1987) indicate that models can not only simulate large scale circulation systems but also study some mesoscale eddies. In particular, for an average flow in the upper ocean, models have a relatively strong capability. A simple model with few factors is very helpful for us to seize the focus and study the mechanism. This study analyzes and discusses the results of a wind stress-driven model in the Pacific. Comparing the results between the assimilation data and the numerical simulation, we may draw the conclusion that the simulation results of the 1.5-layer ocean model are satisfactory.

The governing equations of motion in the 1.5-layer ocean model can be written as follows:

$$\frac{\partial U}{\partial t} - fV = g'(H-h)\frac{\partial h}{\partial x} + \frac{\tau_x}{\rho_0} + A_H\nabla^2 U, \tag{1}$$

$$\frac{\partial V}{\partial t} - fU = g'(H-h)\frac{\partial h}{\partial y} + \frac{\tau_y}{\rho_0} + A_H\nabla^2 V, \tag{2}$$

$$-\frac{\partial h}{\partial t} + \left(\frac{\partial U}{\partial x} + \frac{\partial V}{\partial y}\right) = 0, \tag{3}$$

where $U=(H-h)u$ and $V=(H-h)v$ are the zonal and meridional transports in the upper layer, h is the layer interface displacement, H is the thickness of the upper layer at rest, $f=2\Omega\sin\varphi$ is the Coriolis parameter at the central latitude φ of the model domain, and $\Omega=7.292\times10^{-5}\,\mathrm{s}^{-1}$ is the angular rotation rate of the earth, $g'=g(\rho_2-\rho_1)/\rho_2$ is the reduced gravity for the two layers of densities ρ_1 and ρ_2 with $\rho_2>\rho_1$, τ_x and τ_y are the zonal and meridional components of the surface wind stress acting on the ocean, $\rho_0=1025\,\mathrm{kg\,m}^{-3}$ is the average density of the ocean water, and A_H is the coefficient of horizontal eddy viscosity. We discretize Eqs. (1), (2) and (3) on an Arakawa C-grid using centred-differences in both space and time. The wind stress terms are discretized into zonal and meridional components assuming that τ_x and τ_y are defined at the u-points and v-points respectively. The free-slip condition is applied to the northern and southern boundaries and non-slip boundary condition is used at the coast. A_H is designed to increase linearly from $2500\,\mathrm{m}^2\,\mathrm{s}^{-1}$ to $7000\,\mathrm{m}^2\,\mathrm{s}^{-1}$ from 25°N to the northern boundary to damp spurious coastal Kelvin waves and to suppress the instability in the KC extension region along the artificial northern bound-

ary. In the upper layer ocean g' is set at 0.015 m s^{-2} and the initial upper layer thickness H at 200 m, which is consistent with the corresponding depth and density $25\sigma_\theta$ of SODA assimilation data in the Pacific.

The Ekman transport ($\vec{M}_E=\vec{\tau}\times\vec{k}/\rho_0 f$) is removed from the model. By intuitive judgment, the bifurcation point at the western boundary will be calculated in the model. Most scholars defined the location of bifurcation in terms of the surface current in previous studies, for instance the bifurcation latitude is generally defined as the average latitude of some latitudes with zero meridional velocity at the western boundary. The method of Qiu and Lukas (1996) and Kim *et al.* (2004) is used here, which defines the latitude of bifurcation point in the region where the meridional velocity is zero within two longitudes at the western boundary. Kim *et al.* (2004) mentioned that many factors could affect the NEC. A smooth flow field produced by a simple model can reduce the errors. We use the method of constructor in the calculation by using three points around the minimum value of the original grid points to construct a function and by using Cramer's rule to solve the equations. We obtain the point with the minimum value and use it as the optimal value of the bifurcation latitude. This value makes the change more smooth (no larger jumps) and the data obtained seem more reasonable.

The terrain data from the 5' global ocean depth topographical ETOPO5 of NGDC published by UCAR website are used in the model. Comparing data of different resolutions, we found that the coarse resolution for this simple model is good enough to show bifurcation. We set the terrain data onto 0.5°× 0.5° grids for the calculation. To meet the calculation requirements, the following terrain data for the conceptual model are removed: those corresponding to the parts that are closer to the coast and shallower than 100 m and some unstable single points. The Hawaiian terrain data are reserved. To reduce the effect of the boundary, we will not cut off the complete circulation systems. We take the computational domain (–18.25°S–39.25°N, 120.25°E–288.25°E) for the model.

The average monthly wind stress data are obtained from the SODA monthly wind stress data of the University of Maryland which have a resolution of 0.5°×0.5° and a time range from 1958 to 2007. Another wind stress dataset of the sea surface wind is the monthly data of the European Centre for Medium-Range Weather Forecasts (ECMWF). The time range of the data is from 1958 to 2002 and its resolution is 2.5°×2.5°. The average monthly wind stress is interpolated to the grids of the computational domain. Comparison between the ECMWF wind stress data and the SODA assimilation data shows that they are not significantly different. After testing with the model, it is found that there is no remarkable difference between the results of flow fields forced by the data of ECMWF and SODA. It is known that the SODA wind stress assimilation data includes more refined ECMWF wind stress data. Therefore the SODA wind stress assimilation data will be used in the following study.

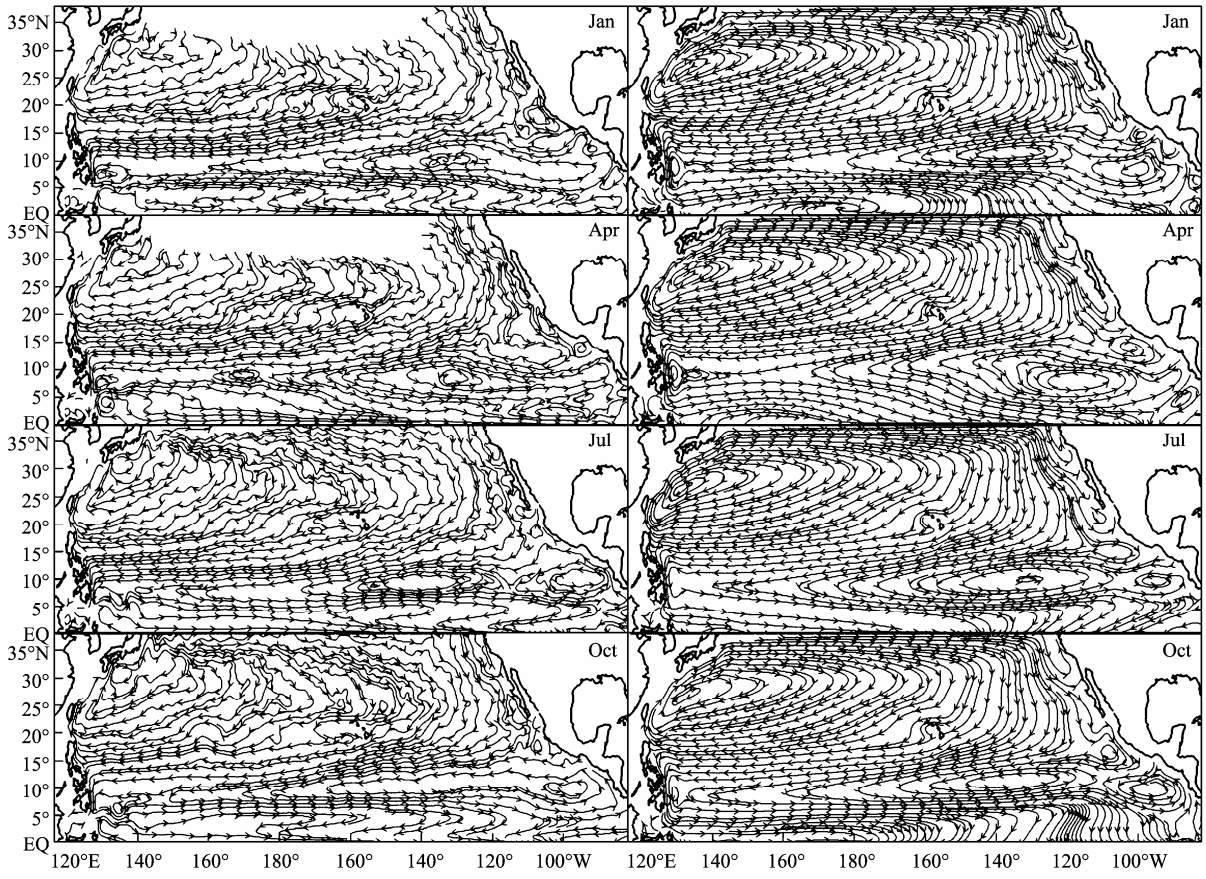

Fig.1 The flow field of SODA isopotential density ($25\sigma_\theta$) (left column) and the results of model driven by the monthly wind stress (right column) (January, April, July, October).

We drive the 1.5-layer model with a given wind stress. The model is run for 20 years so that the energy of the model reaches a steady state, then it is run for another 10 years. The average state in the latter 10 years is used to represent the steady state and seasonal trends. Further experiments are also run according to this approach. Because we are concerned about the distribution of bifurcation at the western boundary and the interior ocean in the North Pacific, an enlargement of the simulated domain is designed to reduce the effects of the north-south boundary. For clearness, only the simulation results of the North Pacific are given here.

The flow field results of the model driven by wind stress and the corresponding SODA assimilation data are given in Fig.1 with January, April, July and November representing winter, spring, summer and autumn, respectively. Fig.1 shows that the model results are smoother than those given by the SODA data. These results show that the bifurcation points at the western boundary are in high latitudes in January and the dual cyclone structure of WWN-EES has been embodied in the two data-sets. It indicates the location of the interior bifurcation is in the east because the western edge of the counterclockwise circulation is in the east in low latitudes over the middle-east Pacific; SODA assimilation data show that the bifurcation at the western boundary moves southward in April, which is also reflected in the model results. In the middle-east Pacific, the circulation center combines two centers into one and its western edge moves westward while the interior bifurcation shows westward movement. Compared with April, the bifurcation point at the western boundary continues to move southward in July and the model results are consistent with the SODA assimilation data. The circulation center of the middle-east Pacific is divided into two again, and the center of large circulation moves westward while the western edge representing the bifurcation moves westward also; In November the bifurcation point at the western boundary is obviously northward and the circulation system of the middle-east Pacific begins to shrink in the eastward direction. The comparison of seasonal variation shows that the main patterns of the circulation system and the changes that correspond with the actual situation are reflected by the model, so the model can meet the requirements of our bifurcation study. The model results are similar with the SODA assimilation data, in the bifurcation characteristics, which indicates that the wind stress is significant to the upper NEC bifurcation and the 1.5-layer model has the capability for describing the major changes of the circulation system in the North Pacific.

3 Results

For understanding the regional wind stress effect about the NEC bifurcation point at the western boundary and the interior bifurcation, we divided the North Pacific into three regions: the Eastern Pacific, the Central Pacific and the Western Pacific. The 15°N, which represents the average latitude of the NEC bifurcation at the western boundary, is taken as the boundary to study the effect of bifurcation at the western boundary and the inner circulation by enhancing (or weakening) wind stress curl in different regions.

The wind stress in the modelling is designed to be a simplified zonal distribution according to the actual long-term average wind stress. It is mainly composed of zonal wind stress that includes three parts. Their curl ($\pm 10^{-7}$ N m^{-3}) zones are separated as tropical and subtropical regions by 15°N. The wind stress decreases to zero from 15°N to the equator. The curl to the south of the equator turns negative, whose value is 1/3 of the north wind stress curl up to the southern boundary. The distribution of wind stress driving the circulation plays the role of an average field with the wind stress anomalies superimposed on it. The curl of the additional wind stress anomalies is 5×10^{-8} N m^{-3} inside of the ellipse and zero outside it, and the wind stress is reduced gradually near the boundary.

In the model, the forcing wind stress is modified as follows:

$$\vec{\tau} = \vec{\tau}_{\text{ave}} + \vec{\tau}_{\text{add}}, \tag{4}$$

where $\vec{\tau}_{\text{ave}}$ is the long-term average wind stress, and $\vec{\tau}_{\text{add}}$ is the additional forcing wind stress for the model. The curl is fixed in the selected region.

The ideal wind stress anomalies (Tomoko and Liu, 2002) for the model are set at fixed latitude and longitude coordinates according to Eq. (5), in which r_0 and mr_0 are the long and short elliptical axes, m is the corresponding scale factor.

$$x^2/r_0^2 + y^2/(mr_0)^2 = 1. \tag{5}$$

When the center and the point of wind stress anomalies are inside of the ellipse, the conditions of the ideal wind stress should be met:

$$\tau^x_{\text{add}} = -ky/r_0^2\ ;\ \tau^y_{\text{add}} = kx/(mr_0)^2. \tag{6}$$

At this point, the curl anomalies produced by wind stress is constant:

$$Curl(\vec{\tau}_{\text{add}}) = \partial\tau^y_{\text{add}}/\partial x - \partial\tau^x_{\text{add}}/\partial y = k(1+m^2)/(mr_0)^2. \tag{7}$$

When the distance from center to the point of wind stress anomalies is on the ellipse and its outside, the additional wind stress follows the relations:

$$\tau^x_{\text{add}} = -ky/(x^2+y^2)\ ;\ \tau^y_{\text{add}} = kx/(x^2+y^2). \tag{8}$$

Thus the curl of wind stress anomalies is

$$Curl(\vec{\tau}_{\text{add}}) = \partial\tau^y_{\text{add}}/\partial x - \partial\tau^x_{\text{add}}/\partial y = 0. \tag{9}$$

By moving the zero line of the curl to different latitudes, the effect on the bifurcation is investigated using the model driven by the ideal wind stress directly.

The zero line of the wind stress curl plays an important role in determining the location of the upper NEC bifurcation point at the western boundary (see Fig.2). The bifurcation point at the western boundary moves northward (southward) as the zero line moves northward (southward). The bifurcation point at the western boundary is

not determined by the zero line completely when the zero line deviates from the average location (15˚N). When the zero line is located at 20˚N, the bifurcation point at the western boundary is located at 18.252˚N; when it is located at 15˚N and 10˚N, the bifurcation point is located at 15.125˚N and 11.246˚N, respectively. When the zero line deviates from the average location a certain bias of latitude between the bifurcation point and the zero line will grow. The bias tends to pull the bifurcation point to the equilibrium position. High latitude water is easier to reach the equator through the interior pathway when the zero line is located at lower latitudes.

The zero line of the ideal wind stress curl is set at 15˚N. The results driven by the superimposed wind stress are shown in Fig.3. The zero line at the western boundary is set to be up warped or down warped. The changes caused by the movements of the zero line of the curl are commensurate with the increase or decrease of the field of the wind stress curl. The results of increasing wind stress curl show that the bifurcation point at the western boundary is

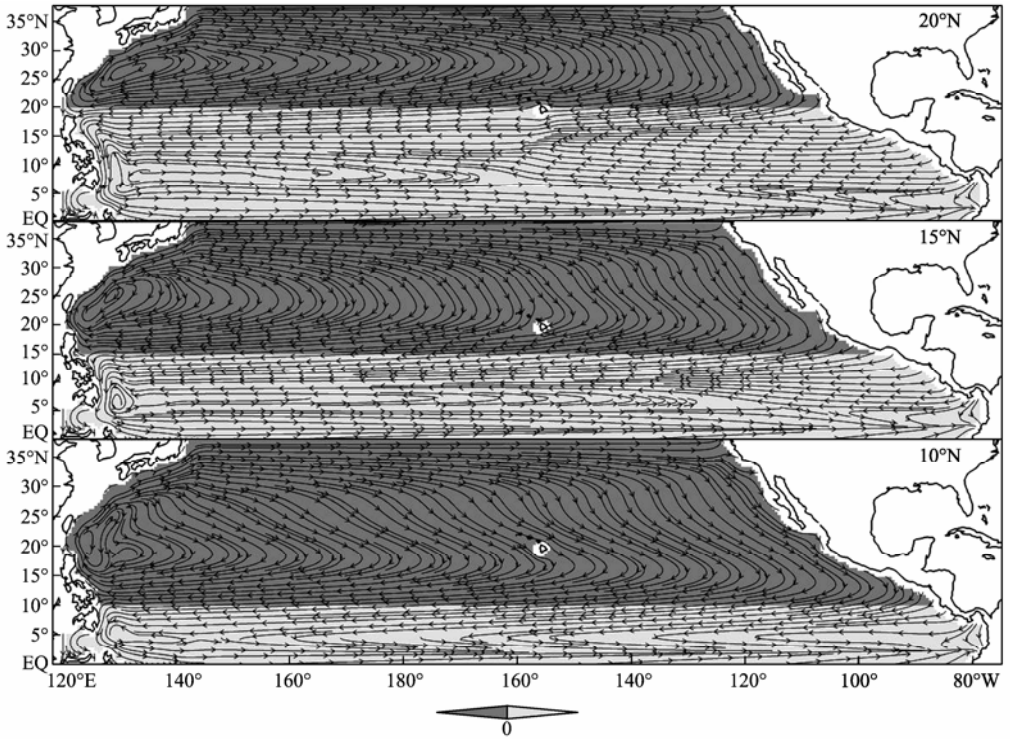

Fig.2 The circulation driven by the ideal wind stress when the zero line of the curl is located at 20˚N, 15˚N and 10˚N, respectively (gray for curl, light color for 1×10^{-7} N m^{-3} and deep color for -1×10^{-7} N m^{-3}).

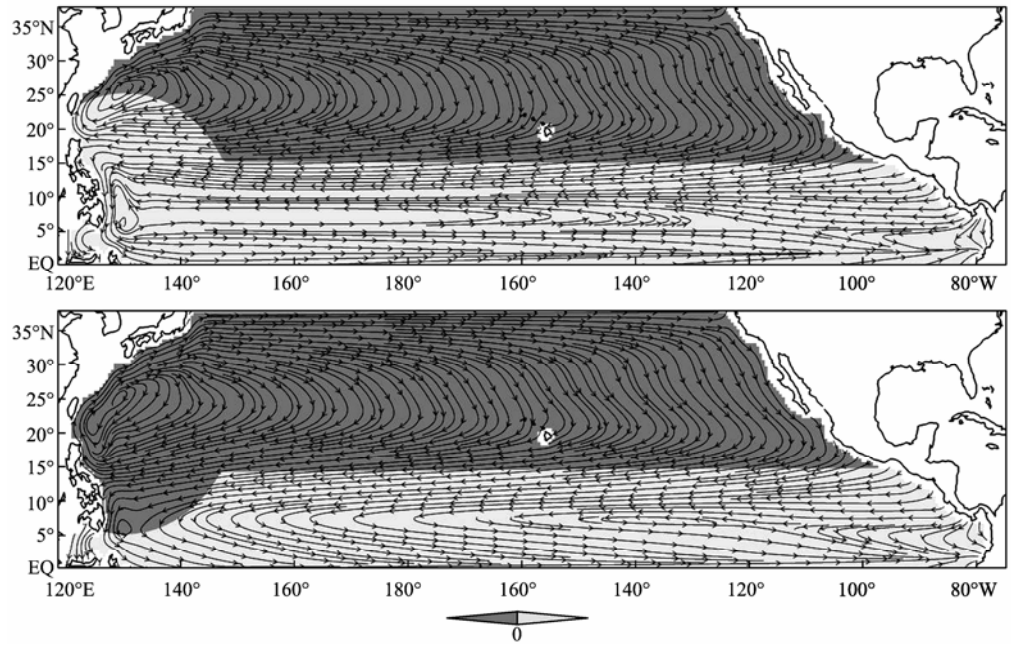

Fig.3 The zero line of wind stress curl moves upward or downward at the western boundary near 15˚N (gray for curl, light color for 1×10^{-7} N m^{-3} and deep color for -1×10^{-7} N m^{-3}).

located at 17.754˚N. The bifurcation point under reduced wind stress curl is located at 12.741˚N. Therefore there is a difference of 5.013˚ between them, or about 2.5˚ off the normal. It indicates that the change of the zero line of the wind stress curl has caused the point to move northward or southward. The trend is that superimposed positive (negative) curl at the western boundary makes the bifurcation point move northward (southward). The change of local wind stress curl will cause the bifurcation point at the western boundary to change. The ME intensity is positively correlated with superimposed curl, which corresponds to the width of interior pathway decreasing (increasing) in the middle-east Pacific at low latitudes.

The region of the superimposed wind stress are divided into six parts and the zero line of the ideal wind stress curl is also set at 15˚N. The six regions are A (0˚–15˚N, 120˚E–170˚E), B (0˚–15˚N, 170˚E–140˚W), C (0˚–15˚N, 140˚W–90˚W), D (15˚N–35˚N, 120˚E–160˚E), E (15˚N–35˚N, 160˚E–160˚W), and F (15˚N–35˚N, 160˚W–120˚W). The anomalous wind stress curl is 5×10^{-8} N m^{-3}.

The circulation driven by the ideal wind stress and the superimposed wind stress anomalies in regions A and F is shown in Fig.4. The situations for regions B, C, D and E are similar to this, so the relevant figures are not given. Fig.4 and Table 1 show that the NEC bifurcation latitude at the western boundary shifts only 0.392˚ for a given zero line of the wind stress curl. Therefore, if the positive and negative curl line does not change, the increased or reduced curl of the wind stress will not cause the NEC bifurcation latitude at the western boundary to change. However, a greater change occurs in the low latitude circulation. The effect of increased or reduced curl will propagate to the western boundary in the form of wave that results in change of the strength of the ME and the middle-east Pacific circulation, causing the interior pathway to change. When the positive wind stress curl is increased in the field, it will promote the development and eastward extention of the ME, and the intensity of the low latitude middle-east Pacific circulation will be reduced, making the interior pathway blocked. When the negative wind stress curl strengthens, it will produce waves propagating to the western boundary and making the ME weaken and move back westward. Thus the intensity of the middle-east Pacific circulation strengthens at low latitudes, and then the interior pathway tends to be clear.

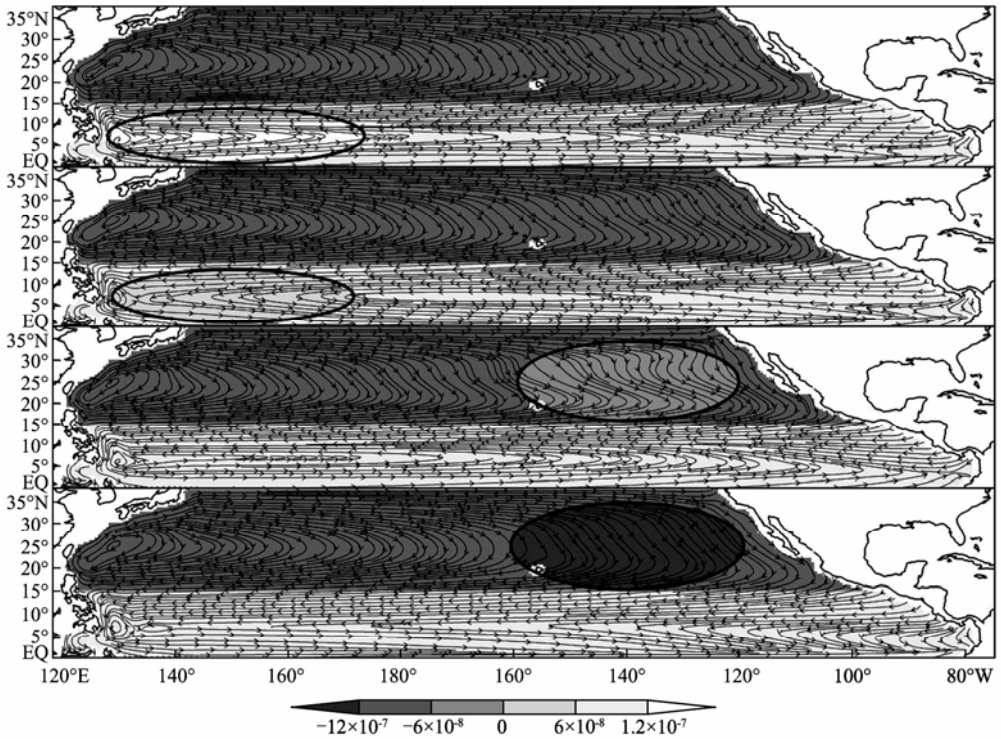

Fig.4 The circulation driven by the ideal wind stress and superimposed anomalies in regions A and F (gray for curl, the interval is 6×10^{-8} N m^{-3}).

Table 1 The bifurcation latitudes at the western boundary forced by the wind stress in different regions

Region with superimposed wind stress	A	B	C	D	E	F
When positive curl is added	14.755	14.865	14.698	14.624	14.744	14.656
When negative curl is added	14.734	14.473	14.810	14.681	14.710	14.808

Fig.5 shows the results with the wind stress curl anomalies superimposed in regions C and F simultaneously. The numerical experiments show whether the configuration in the regions C and F is, respectively, negative and positive, or positive and negative, or positive and positive, or negative and negative, and whether the movement of the bi-

furcation latitude at the western boundary is not significant and the bifurcation is located at the zero line of the wind stress curl when the location of the zero line of curl remains unchanged. But when the positive curl is superimposed, it will make the Rossby wave spread to the western boundary, strengthening the energy of the ME. When the local wind stress curl decreases, the NEC reaches to the equatorial region through the interior pathway easily. When the local wind stress curl increases, the contrary is the case. The configurations of the positive and negative wind stress curl play different roles in the tropical circulation system.

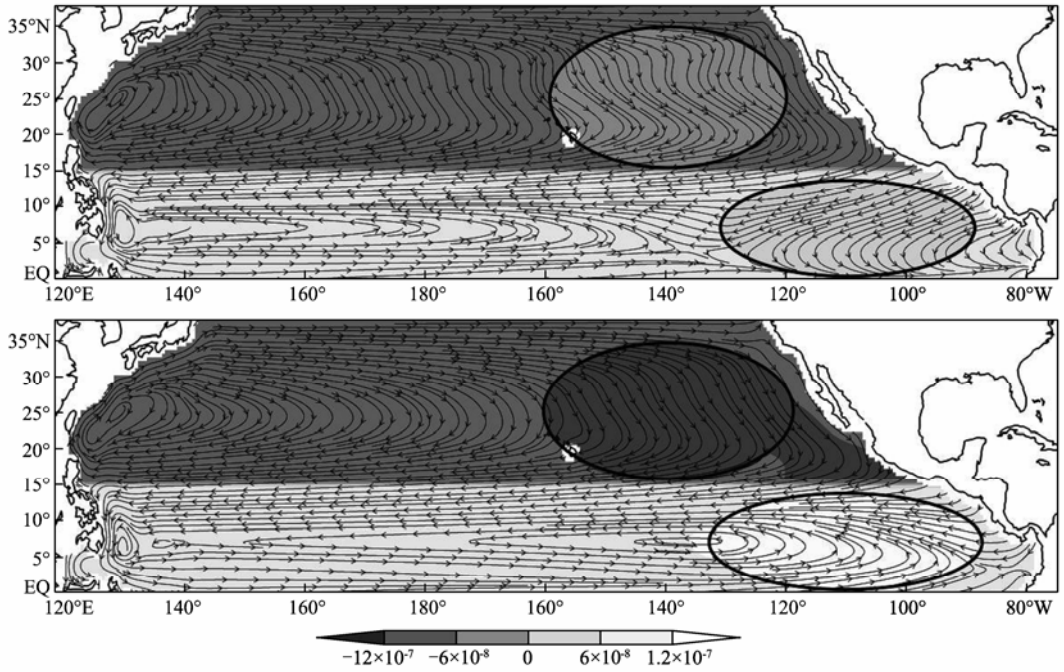

Fig.5 The circulation driven by the ideal wind stress and two superimposed wind stress anomalies in regions C and F (gray for curl, the interval being 6×10^{-8} N m^{-3}).

4 Summary

In this study, the model results we obtain are similar to the actual long-term average and seasonal variation of the flow field and the bifurcation by debugging the wind-stress-driven 1.5-layer model. We study the bifurcation through analyzing the response of the flow field under different configurations of wind stress forcing. The results are as follows:

1) Using climatic wind stress of the SODA data to drive the model till the steady state. The location of the NEC bifurcation point at the western boundary moves northward (southward) in December (June) under the wind stress forcing. The easternmost (westernmost) location of the interior bifurcation of the NEC occurs in October (May). Therefore, the NEC bifurcations at the western boundary and in the interior ocean caused by wind stress are consistent in their seasonal change. The change of westernmost location of the inner bifurcation is ahead of the change of the western boundary by 1–2 months.

2) The ocean circulation forced by the ideal wind stress shows that the zero line of wind stress curl plays a decisive role in the location of NEC bifurcation at the western boundary. The movement of zero line of wind stress curl will determine the location of the NEC bifurcation point at the western boundary. As for the tropical eastern Pacific, the zero line of wind stress curl at lower latitudes is conducive to making the interior pathway clear.

3) In the wind-stress-driven modelling, the increase (decrease) of wind stress curl on the zero line causes the NEC bifurcation point at the western boundary to move northward (southward) slightly. The increase (decrease) of wind stress curl over the flow field will enhance (reduce) the ME but reduce (enhance) the circulation at low latitudes in the middle-east Pacific by the westward propagation of Rossby wave that decreases (increases) the width of interior pathway. The enhanced or reduced ME is one of the important factors of the bifurcation movement. The zonal increase (decrease) of the ME makes the interior pathway narrow (broaden) and the westernmost point of bifurcation move eastward (westward), while its meridional extension (restriction) causes the bifurcation point at the western boundary to move northward (southward), and the changes of the ME are affected by the wind stress curl significantly.

Acknowledgements

This study is supported by the National Natural Science Foundation of China (Nos. 40876004 and 40890155) and the National Basic Research Program of China (973 Program) (No. 2007CB411801). We would like to express our thanks to the University of Maryland and Texas A&M University for their providing the SODA data and

to UCAR who provides the 5' global ocean depth topographical ETOPO5. We also thank all the others who have helped us.

References

Cai, S. Q., Liu, H. L., Li, W., and Long, X. M., 2005. Application of LICOM model to the numerical study of the water exchange between the South China Sea and its adjacent oceans. *Acta Oceanologica Sinica*, **24** (4): 10-19.

Chen, Z. H., and Wu, L. X., 2011. Dynamics of the seasonal variation of the North Equatorial Current bifurcation. *Journal of Geophysical Research*, 116, C02018, Doi: 10.1029/2010-JC006664.

Chu, T. Y., 1972. A study on the water exchange between Pacific Ocean and the South China Sea. *Acta Oceanographica Taiwanica*, **2**: 11-24.

Dale, W. L., 1956. Wind and drift currents in the South China Sea. *The Malayan Journal of Geography*, **8**: 1-31.

Fine, R., Lukas, R., Bingham, F. M., Warner, M. J., and Gammon, R. H., 1994. The western equatorial Pacific is a water mass crossroads. *Journal of Geophysical Research*, **99**: 25 063-25 080.

Gordon, A. L., 1986. Interocean exchange of thermocline water. *Journal of Geophysical Research*, **91**: 5037-5046.

Han, Y. J., 1984. A numerical world ocean general circulation mode1, Part I. Basic design and barotropic experiment. *Dynamics of Atmospheres and Oceans*, **8**: 107-141.

Huang, Q. Z., 1983. Variations of velocity and transport of the kuroshio in the bashi channel. *Journal of Tropical Oceanography*, **2** (1): 35-40 (in Chinese with English abstract).

Johnson, G. C., and McPhaden, M. J., 1999. Interiod pycnocline flow from the Subtropical to the Equatorial Pacific Ocean. *Journal of Physical Oceanography*, **29**: 3073-3089.

Kessler, W. S., and Taft, B. A., 1987. Dynamic height and zonal geostrophic transports in the central Pacific during 1979–84. *Journal of Physical Oceanography*, **17**: 97-122.

Kim, Y. Y., Qu, T. D., Jensen, T., Miyama, T., Mitsudera, H., Kang, H.-W., and Ishida, A., 2004. Seasonal and interannual variations of the North Equatorial Current bifurcation in a high-resolution OGCM. *Journal of Geophysical Research*, **109**, C03040, Doi: 10.1029/2003JC002013.

Li, K. R., Lin, X. C., and Wu, Z. X., 1996. The features of mean wind stress field in the pacific ocean. *Acta Geographica sinica*, **51** (1): 25-32 (in Chinese with English abstract).

Li, L. J., Liu, Q. Y., and Liu, W., 2005. Surface speed and bifurcation of the North Pacific Current in the Pacific ocean. *Journal of Ocean University of China*, **35** (3): 370-374 (in Chinese with English abstract).

Li, L., Nowlin, W. D., and Su, J. L., 1998a. Anticyclonic rings from the Kuroshio in the South China Sea. *Deep Sea Research Part I*, **45**: 1 469-1 482 (in Chinese with English abstract).

Li, W., Liu, Q. Y., and Xu, Q. Y., 1994. The effect of the sst anomaly in the north pacific due to the meander of the kuroshio in winter on the low frequency oscillation. *Journal of Ocean University of Qingdao*, **24** (4): 447-454 (in Chinese with English abstract).

Li, W., Liu, Q. Y., and Yang, H. J., 1998b. Principal features of ocean circulation in the luzon strait. *Journal of Ocean University of Qingdao*, **28** (3): 345-352 (in Chinese with English abstract).

Lighthill, M. J., 1969. Dynamic response of the Indian Ocean to onset of the southwest monsoon. *Philosophical Transactions of the Royal Society of London A*, **265**: 45-92.

Liu, Q. Y., Liu, C. T., Zheng, S. P., Xu, Q. C., and Li, W., 1996. The deformation of Kuroshio in the Luzon Strait and its dynamics. *Journal of Ocean University of Qingdao*, **26** (4): 413-420 (in Chinese with English abstract).

Liu, Q. Y., Pan, A. J., and Liu, Z. Y., 2003. Intraseasonal oscillation and baroclinic instability of upper layer ocean in the north equator current. *Oceanologia and limnologia sinica*, **34** (1): 94-100 (in Chinese with English abstract).

Liu, Z., 1994. A simple model of the mass exchange between the subtropical and tropical ocean. *Journal of Physical Oceanography*, **24**: 1153-1165.

Lu, P., McCreary, J. P., and Klinger, B. A., 1998. Meridional circulation cell and the source water of the Pacific equatorial undercurrent. *Journal of Physical Oceanography*, **28**: 62-84.

Masumoto, Y., and Yamagata, T., 1991. Response of the Western Tropical Pacific to the Asian Winter Monsoon: The generation of the Mindanao Dome. *Journal of Physical Oceanography*, **21**: 1386-1398.

Masuzawa, J., 1968. Second cruise for CSK, Ryofu Maru, January to March 1968. *Oceanographic Magazine*, **20**: 173-185.

McCreary, J. P., and Lu, P., 1994. On the interaction between the subtropical and equatorial ocean circulation:the Subtropical Cell. *Journal of Physical Oceanography*, **24**: 466-497.

Metzger, E. J., and Hurlburt, H. E., 1996. Coupled dynamics of the South China Sea, the Sulu Sea, and the Pacific Ocean. *Journal of Geophysical Research*, **101**: 12 331-12 352.

Metzger, E. J., and Hurlburt, H. E., 2001. The nondeterministic nature of Kuroshio penetration and eddy shedding in the South China Sea. *Journal of Physical Oceanography*, **31** (7): 1712-1732.

Munk, W. H., 1950. On the wind-driven ocean circulation. *Japan Journal of Meteorology*, **7**: 79-93.

Nitani, H., 1972. *Beginning of the Kuroshio. Kuroshio, Physical Aspects of the Japan Current*. University of Washington Press, Washington, USA, 129-163.

Qiu, B., and Chen, S., 2010. Interannual-to-decadal variability in the bifurcation of the North Equatorial Current off the Philippines. *Journal of Physical Oceanography*, **40**: 2525-2538.

Qiu, B., and Lukas, R., 1996. Seasonal and interannual variability of the North Equatorial Current, the Mindanao Current, and the Kuroshio along the Pacific western boundary. *Journal of Geophysical Research*, **101**: 12 315-12 330.

Qu, T. D., and Lukas, R., 2002. Depth distribution of the subtropical Gyre in the North Pacific. *Journal of Oceanography*, **58** (3): 525-529.

Qu, T. D., and Lukas, R., 2003. The bifurcation of the North Equatorial Current in the Pacific. *Journal of Physical Oceanography*, **33**: 5-18.

Qu, T. D., Meyers, J. G., and Godfrey, S., 1997. Upper ocean dynamics and its role in maintaining the annual mean western Pacific warm pool in a global GCM. *International Journal of Climatology*, **17**: 711-724.

Qu, T. D., Mitsuder, A. H., and Yamagata, T., 2000. Intrusion of the North Pacific waters into the South China Sea. *Journal of Geophysical Research*, **105** (c3): 6415-6424.

Qu, T. D., Mitsudera, H., and Yamagata, T., 1998. On the western boundary currents in the Philippine Sea. *Journal of Geophysical Research*, **103** (4): 7537-7548.

Qu, T. D., Mitsudera, H., and Yamagata, T., 1999. A climatology of the circulation and water mass distribution near the

Philippine coast. *Journal of Physical Oceanography*, **29**: 1488-1505.

Schott, G., 1939. Die äquatorialen Strömungen des westlichen Stillen Ozeans. *Annalen der Hydrographie und Maritimen Meteorologie*, **67**: 247-257 (in German).

Stommel, H. M., 1948. The westward intensification of wind driven ocean currents. *Transactions, American Geophysical Union*, **29**: 202-206.

Stommel, H., and Yoshida, K., 1972. *Bathymetry of the Kuroshio Region*. University of Tokyo Press, Tokyo, Janpan, 53-80.

Su, J. L., and Yuan Y. L., 2005. *Coastal Hydrology in China*. Ocean Press, Beijing, China, 250-296 (in Chinese).

Sverdrup, H. U., 1947. Wind-driven currents in a baroclinic ocean with application to the equatorial currents of the eastern Pacific. *Proceedings of the National Academy of Sciences*, **33**: 318-326.

Takahashi, T., 1959. Hydrographical researches in the western equatorial Pacific. *Memoirs of the Faculty of Fisheries, Kagoshima University*, **7**: 141-147.

Tomoko, I., and Liu Z. Y., 2002. Mid-latitude wind forcing and subduction of temperature anomalies. *Journal of Physical Oceanography*, **32**: 1094-1105.

Toole, J. M., Millard, C., Wang, Z., and Pu, S., 1990. Observations of the Pacific North Equatorial Current bifurcation at the Philippine coast. *Journal of Physical Oceanography*, **20**: 307-318.

Toole, J. M., Zou, E., and Millard, R. C., 1988. On the circulation of the upper waters in the western equatorial Pacific Ocean. *Deep Sea Research Part A*, **35**: 1451-1482.

Tsuchiya, M., 1968. Upper waters of the intertropical Pacific Ocean. *Johns Hopkins Oceanographic Studies*, **4**: 50.

Wajsowicz, R. C., 1999. Variations in gyre closure at the water mass crossroads of the western equatorial Pacific Ocean. *Journal of Physical Oceanography*, **29**: 3002-3024 (in Chinese with English abstract).

Wang, Q. Y., and Hu, D. X., 2006. Bifurcation of the North Equato-rial Current derived from altimetry in the Pacific Ocean. *Journal of Hydrodynamics*, **18** (5): 620-626.

Wang, Q. Y., Cao, R. X., Zhang, S. W., and Hu, D. X., 2009. Surface bifurcation of the NEC in the Pacific Ocean. *Science in China (Series D)*, **39** (1): 116-120 (in Chinese).

Wang, Q., and Liu, Q. Y., 2000. The study on the pacidic subtropical cell. *The National Science Foundation of China*, **1**: 1-5 (in Chinese with English abstract).

Wang, W., and Su, J. L., 1987. A barotropic model about the Kuroshio system and the vortex phenomenon in Yellow Sea and East Sea. *Acta Oceanlogica Sinica*, **9** (3): 271-275 (in Chinese with English abstract).

Webster, P. J., and Lukas, R., 1992. TOGA/COARE: The coupled ocean-atmosphere response experiment. *Bulletin of the American Meteorological Society*, **73** (9): 1377-1416.

Wyrtki, K., 1961. Physical oceanography of the southeast Asian waters. NAGA Report Vol. 2, University of California, 195pp.

Yaremchuk, M., and Qu, T. D., 2004. Seasonal variability of the large-scale currents near the coast of the Philippines. *Journal of Physical Oceanography*, **34** (4): 844-855.

Ye, A. L., and Li, F. Q., 1992. *Physical Oceanography*. Ocean University of Qingdao Press, Qingdao, China, 684pp (in Chinese).

Yuan, D. L., 2002. Dynamics of the Luzon Strait transports. *Acta Oceanologica Sinica*, **21** (2): 175-185.

Zeng, Q. C., Ji, Z. Z., and Li, R. F., 1985. A numerical offshore current model and dectection. *Journal of Hydrodynamics*, **2** (1): 67-71 (in Chinese with English abstract).

Zhang, X. D., Xiu, Y. R., Liu, J. F., Su, G., and Wang, Q. Y., 2008. The determination about the NEC and its bifurcation latitude of the variations. *Marine Forecasts*, **25** (2): 33-41 (in Chinese with English abstract).

(Edited by Xie Jun)